

# The Exact Solution of an Octagonal Rectangle Triangle Random Tiling

Jan de Gier      Bernard Nienhuis

*Instituut voor Theoretische Fysica, Universiteit van Amsterdam,  
Valckenierstraat 65, 1018 XE Amsterdam, The Netherlands*

## Abstract

We present a detailed calculation of the recently published exact solution of a random tiling model possessing an eight-fold symmetric phase. The solution is obtained using Bethe Ansatz and provides closed expressions for the entropy and phason elastic constants. Qualitatively, this model has the same features as the square-triangle random tiling model. We use the method of P. Kalugin, who solved the Bethe Ansatz equations for the square-triangle tiling, which were found by M. Widom.

Key words: quasi-crystals, random tilings, Bethe Ansatz, exact solution.

# 1 Introduction

Random tiling models are ensembles of coverings of the plane, without gaps or overlaps, with a set of rigid building blocks or tiles. The most well-known application of such a model is perhaps the anti-ferromagnetic Ising model on the triangular lattice,<sup>(1)</sup> of which the ground state configurations are described by rhombus coverings of the plane.

The discovery of quasi-crystals<sup>(2)</sup> revived the modeling of structures by tiling models.<sup>(3)</sup> Quasi-crystals are solid metallic alloys without periodicity but with long range order (i.e. they have sharp diffraction peaks). Two competing scenarios have been put forward to explain the origins of such quasiperiodic ordering. One of them assumes a microscopic Hamiltonian of which the ground state configuration is quasi-periodic. This would be something akin to the local matching rules used by Penrose. These deterministic tilings are perfectly quasiperiodic in the sense that their diffraction peaks have zero width. As an alternative there is the random tiling picture, in which one abandons the strict quasiperiodic long range order. These models do have matching rules in the sense that tiles may neither overlap nor have gaps between them, but these are not strong enough to enforce a unique behavior at large distances. This then gives rise to an ensemble of different tilings, or atom packings, inside a fixed volume. Assuming that all these configurations are (nearly) degenerate in energy such an ensemble has a nonzero entropy density. This entropy can reduce the free energy and lower it w.r.t the crystalline phase, which is supposed to be stable at zero temperature. This phenomenon thus provides a simple explanation of the stability of the quasi-crystalline phase.

Of special interest in two dimensional random tiling models are those that fulfill the following constraints: (i) each kind of tile has a unique atomic decoration, (ii) each member of the random tiling ensemble is an allowed packing of atoms and (iii) each arrangement of atoms forming an equally good packing belongs to the tiling ensemble. These tiling models are called physical or atomistic. Examples of these are the binary tenfold rhombus<sup>(4)</sup> and the twelve-fold square-triangle<sup>(5,6)</sup> random tiling models. Recently Cockayne introduced a physical random tiling model with an eight-fold symmetric phase which he doped the octagonal analogue of the square-triangle tiling, despite of some distinctive characteristics.<sup>(7)</sup> In this paper we show that the comparison certainly holds concerning the exact solvability of the random

tiling model. We mean by this that, like for the square-triangle tiling,<sup>(8,9)</sup> it is possible to calculate the entropy exactly in part of the phase diagram. We obtain closed expressions for the residual entropy as well as for the phason elastic constants.<sup>(10)</sup> The main results of this paper have already been published elsewhere,<sup>(11)</sup> here we present the full calculation.

The paper is organized as follows: In section 2 we present the tiling model and give a transfer matrix description to be able to enumerate all possible tilings. In section 3 we give a brief review of phason strain concepts. The results of this section will be used to identify our results and to obtain expressions for the phason elastic constants. Section 4 describes the diagonalization of the transfer matrix by Bethe Ansatz. The resulting nonlinear coupled equations are solved in section 5. Finally we calculate the entropy density from this solution in section 6.

## 2 The square-hexagon tiling and the transfer matrix

The model that Cockayne described is a tiling of the plane by squares and various hexagons. By placing discs of radius  $1/2$  on each of the vertices, one obtains a physical packing. The hexagons can be thought of as being built out of two isosceles triangles and several rectangles depending on the length of the hexagon. The rectangles have sides  $1$  and  $\sqrt{2}$ . Likewise, by drawing one of the two diagonals, the squares can be viewed as two triangles. The square-hexagon tiling thus is equivalent to the ensemble of vertex configurations of the rectangle-triangle tiling. The latter ensemble in turn is equivalent to the rectangle-triangle random tiling ensemble (see Fig. 1) provided that the two ways of forming a square out of two triangles are counted as one.<sup>(11)</sup>

Like for the square-triangle tiling we make use of the transfer matrix to calculate thermodynamic quantities like the entropy. The transfer matrix  $\mathbf{T}$  is introduced by decomposing the tiling into layers. Different layers are bounded by the short horizontal edges, the horizontal diagonals of the squares and the almost horizontal diagonals of the  $\pm\pi/4$  tilted rectangles. Here,  $\pm$  refers to the tilt of the short edge of the rectangle w.r.t the horizontal axis. In addition, the layer boundaries cut the triangles and rectangles with a vertical long edge in half. The horizontal diagonals of the squares are denoted by the

dashed lines in Fig. 1. In a similar fashion the tiling can be decomposed in ‘columns’. Different columns are separated by the short + edge, the vertical short edge and the almost vertical diagonal of the – tilted rectangle. The rectangles with a vertical long edge are cut by a column edge from the lower left to the upper right corner. In this way the tiles are deformed in such a way that the vertices of the tiling form a subset of those of the square lattice, see Fig. 2.

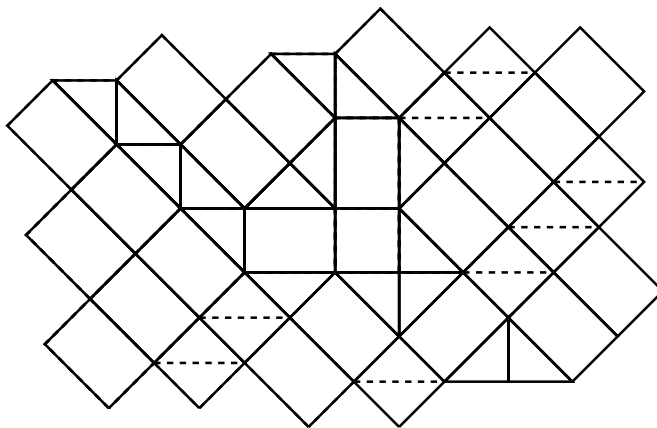


Figure 1: Patch of the tiling model. The diagonals of the squares are not drawn. Dashed lines indicate parts of the layer boundaries.

On this regular lattice the definition of the transfer matrix  $\mathbf{T}$  is obvious: a matrix element  $T_{ij}$  is 0 if layer  $j$  can not be followed by layer  $i$ . Otherwise it is given by the statistical weight of layer  $i$ . In this paper we shall adopt the convention that  $\mathbf{T}$  acts in the downward direction.

In the following we will call the tilted rectangles  $R_{\pm}$  and the rectangles with the short and long horizontal edge by  $R_s$  and  $R_l$  respectively. Because different tiles of the original tiling are mapped onto the same shapes on the square lattice, we have to decorate the new configurations. This is done with bold dashed and solid lines, see Fig. 2. Thus it is apparent that the horizontal short and long edges of the original tiling form domain walls between regions of  $R_+$ , which we denote by type s and l respectively. If we think of the vertical coordinate as a time coordinate (increasing in the downward direction), the transfer matrix can be seen as an evolution operator for these domain walls.

The transfer matrix  $\mathbf{T}$  is block diagonal with sectors parameterized by the numbers of domain walls, which are conserved under the action of  $\mathbf{T}$ .

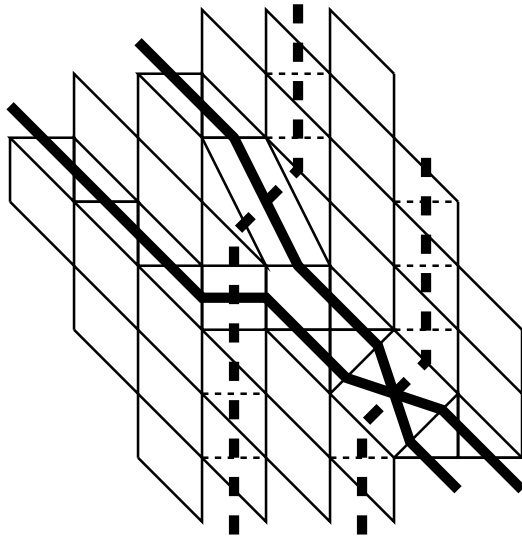


Figure 2: Corresponding patch on the lattice. Bold solid lines are domain walls of horizontal short edges, referred to as s-walls in the text. Bold dashed lines represent the l-walls of horizontal long edges.

Between two layer edges on the square lattice, the s-walls step one unit to the right and the l-walls do not move. When two walls cross, the s-wall may either jump over the l-wall moving two places to the right and thereby creating a rectangle  $R_l$ , or, over *two* layers, the walls may exchange place creating a rectangle  $R_s$ . In the latter case the crossing therefore is completed after application of the transfer matrix twice. It may also happen that two walls of type s and one of type l cross simultaneously over two layers. The l-wall and the s-wall nearest to it then exchange place, while the second s-wall jumps over both these walls moving three places to the right creating a rectangle  $R_-$ .

We can express the tile densities in terms of the domain wall densities. We shall denote the horizontal size of the tiling by  $L$  and the corresponding system size of the lattice model by  $N$ . Let  $\Delta_{ls} = n_{R_l} - n_{R_s} = 0$ , i.e. both types of collisions of two domain walls occur with the same frequency, and

let  $2n_s$  and  $n_l$  be the number of s- and l-walls. Apply the transfer matrix  $p = 2N - 2n_s$  times on some initial configuration of domain walls at  $t = 0$  on the lattice, and suppose that both types of collisions occur for every *pair* of s- and l-walls. The final state at  $t = 2N - 2n_s$  will then be the same configuration of domain walls as the initial one shifted by  $-2n_s$ . Counting the total number of tiles in this patch generated by  $\mathbf{T}$ , we find the following relations between the wall densities and the rectangle densities per layer:

$$p(n_{R_1} + n_{R_s} + 2n_{R_-}) = 2p(n_{R_s} + n_{R_-}) = 4n_s n_l. \quad (1)$$

$$\Delta_{\pm} \equiv n_{R_+} - n_{R_-} = N - 2n_s - n_l. \quad (2)$$

Similar expressions can be obtained for the different triangle densities. The total number of rectangles and of triangles per layer can then be calculated to be:

$$\begin{aligned} n_{\text{rect}} &= N - 2n_s - n_l + 4n_s n_l / p. \\ n_{\text{tri}} &= 2(2n_s + n_l) - 12n_s n_l / p. \end{aligned} \quad (3)$$

The tile densities that belong to the quasi-crystalline phase are  $n_{\text{rect}}/N = 6 - 4\sqrt{2}$ ,  $n_{\text{tri}}/N = 12\sqrt{2} - 16$ , corresponding to an area fraction of triangles  $\alpha_t = 1/2$ . As a function of the domain wall densities, the model displays two incommensurate phases. A four-fold symmetric phase is formed in the high density region,  $\alpha_t > 1/2$ , where the triangles form octagonal and square cells bounded by domain walls consisting of rectangles. There is a two-fold symmetric phase in the low density region where the rectangles form rectangular cells bounded by the domain walls consisting of triangles.

As already mentioned above, the quantities  $n_s$  and  $n_l$  are conserved by the action of the transfer matrix  $\mathbf{T}$ . To control the average value of  $\Delta_{\text{ls}}$ , the tiles  $R_s$  and  $R_l$  are given a weight  $\exp(-\phi)$  and  $\exp(\phi)$  respectively. Furthermore, as the tiles  $R_s$  and  $R_-$  in the lattice representation have an area that is twice that of the other two transformed rectangles, we have to introduce a chemical potential for them to compensate for this asymmetry. The tiles  $R_s$  and  $R_-$  therefore get an extra weight  $\exp(\eta)$ .

The free energy per layer of the lattice model is given by the logarithm of the largest eigenvalue of  $\mathbf{T}$ :

$$\begin{aligned} f(n_s, n_l, \phi) &= -\log \Lambda \\ &= -N\sigma_N - \phi\Delta_{\text{ls}} - \eta(n_{R_s} + n_{R_-}), \end{aligned} \quad (4)$$

where  $\sigma_N$  is the entropy per site of the lattice model. In section 4 will be shown that we can actually diagonalize  $\mathbf{T}$  using coordinate Bethe Ansatz.

### 3 Phason strain

In this section we will briefly review some of the phason strain concepts. Details can be found in a review on random tiling concepts by Henley.<sup>(10)</sup>

The position of every vertex in the tiling is of the form:

$$\mathbf{r} = \sum_{j=0}^3 n_j \mathbf{e}_j^{\parallel}, \quad n_j \in \mathbb{N}. \quad (5)$$

$$\mathbf{e}_j^{\parallel} = (\cos \pi j/4, \sin \pi j/4).$$

The tiling can therefore naturally be embedded in a four-dimensional hypercubic lattice using

$$(\mathbf{r}, \mathbf{h}) = \sum_{j=0}^3 n_j (\mathbf{e}_j^{\parallel}, \mathbf{e}_j^{\perp}), \quad (6)$$

$$\mathbf{e}_j^{\perp} = (\cos 5\pi j/4, \sin 5\pi j/4).$$

The vectors  $\mathbf{e}_j^{\perp}$  are chosen such that  $\mathbf{e}_j = (\mathbf{e}_j^{\parallel}, \mathbf{e}_j^{\perp})$  are orthogonal. The continuous height field, or representative surface,  $\mathbf{h}(\mathbf{r})$  is as horizontal as possible for a perfect quasi-crystalline tiling. A generic member of the random tiling ensemble thus is described by fluctuations around this flat surface. By integrating out the short-wavelength fluctuations one gets a smoothed function  $\mathbf{h}(\mathbf{r})$ , the phason field, that varies on length scales much larger than the tile edge length. The phason strain tensor then is defined by linearization:

$$\mathbf{E} = \nabla_{\mathbf{r}} \tilde{\mathbf{h}}(\mathbf{r}). \quad (7)$$

The macroscopic quasi-crystalline state corresponds to  $\mathbf{E} = 0$ . The random tiling hypotheses now states that the entropy density  $\sigma_a(\mathbf{E}) = S(\mathbf{E})/A$  has its maximum at  $\mathbf{E} = 0$  and that it is quadratic in  $\mathbf{E}$  near  $\mathbf{E} = 0$  for any maximally random tiling. Like the square-triangle tiling, the octagonal tiling has the irrotational property.<sup>(12)</sup> This implies that the most general quadratic form of the entropy density  $\sigma_a$  consistent with 8-fold rotational symmetry is

$$\sigma_a = \sigma_{a,0} - \frac{1}{2} K_{\mu} (\text{Tr} \mathbf{E})^2 + \frac{1}{2} K_{\xi} \det \mathbf{E} + \mathcal{O}(\mathbf{E}^3) \quad (8)$$

We denote the deviations of the quasi-crystalline densities by

$$\begin{aligned} \delta_{\text{ls}} &= n_l \sqrt{2} - 2n_s, \\ \Delta_{\pm} &= N - n_l - 2n_s. \end{aligned} \quad (9)$$

The quadratic forms in (8) can be expressed in these, using  $L = n_1\sqrt{2} + 2n_s$

$$\begin{aligned} (\text{Tr}\mathbf{E})^2 &= \frac{1}{L^2} \left( 2\delta_{\text{ls}} - \Delta_{\pm}(2 - \sqrt{2}) - \Delta_{\text{ls}}(1 + \sqrt{2}) \right)^2. \\ \det \mathbf{E} &= \frac{1}{L^2} \left( \delta_{\text{ls}}^2 - (2 - \sqrt{2})\Delta_{\pm}\delta_{\text{ls}} - 2\Delta_{\pm}^2\sqrt{2} \right. \\ &\quad \left. - (1 + \sqrt{2})\Delta_{\text{ls}}(\delta_{\text{ls}} - (1 - \frac{1}{2}\sqrt{2})\Delta_{\pm}) \right). \end{aligned} \quad (10)$$

The conditions on the elastic constants for  $\mathbf{E} = 0$  to be a local maximum of  $\sigma_a$  are:

$$K_{\mu} > 0, \quad K_{\xi} > 0, \quad 4K_{\mu} - K_{\xi} > 0. \quad (11)$$

## 4 Bethe Ansatz

It is possible to diagonalize the transfer matrix by making an Ansatz for its eigenvectors. Details of this so-called Bethe Ansatz are given in Appendix A. A technical point we mention here is the fact that the s-walls split up in two different species, odd and even ones, both of which are conserved under the action of  $\mathbf{T}$ . Their densities are given by  $n_o$  and  $n_e$  respectively, with  $n_o + n_e = 2n_s$ . The eigenvectors and eigenvalue can be expressed in three sets of complex numbers corresponding to the three different kinds of domain wall. The eigenvalue is given by

$$\Lambda = \prod_{i=1}^{n_o} u_i \prod_{j=1}^{n_e} v_j, \quad (12)$$

if the numbers  $u_i$  and  $v_j$  satisfy the following equations

$$\begin{aligned} u_i^N &= (-)^{n_o-1} \prod_{k=1}^{n_1} (e^{\phi} u_i + e^{\eta-\phi} u_i^{-1} w_k^{-1}). \\ v_j^N &= (-)^{n_e-1} \prod_{k=1}^{n_1} (e^{\phi} v_j + e^{\eta-\phi} v_j^{-1} w_k^{-1}). \\ w_k^{-N} &= (-)^{n_1-1} \prod_{i=1}^{n_o} (e^{\phi} u_i + e^{\eta-\phi} u_i^{-1} w_k^{-1}) \prod_{j=1}^{n_e} (e^{\phi} v_j + e^{\eta-\phi} v_j^{-1} w_k^{-1}). \end{aligned} \quad (13)$$



The equations (13) are the Bethe Ansatz equations (BAE). Using the substitution

$$\xi_{e,j} = v_j^2, \quad \xi_{o,i} = u_i^2, \quad \psi_j = -w_j^{-1}e^{\eta-2\phi}, \quad (14)$$

their logarithmic version can be written as

$$\begin{aligned} \frac{N+n_l}{2}F_s(\xi_{o,i}) &= 0 \pmod{2\pi i}, \\ \frac{N+n_l}{2}F_s(\xi_{e,i}) &= 0 \pmod{2\pi i}, \\ NF_1(\psi_j) &= 0 \pmod{2\pi i}, \end{aligned} \quad (15)$$

where we have defined the following functions

$$F_s(z) = \log(z) - \frac{2}{N+n_l} \sum_{j=1}^{n_l} \log(z - \psi_j) - \frac{2n_l}{N+n_l} \phi. \quad (16)$$

$$\begin{aligned} F_1(z) &= \log(-z) - \frac{1}{N} \sum_{i=1}^{n_o} \log(\xi_{o,i} - z) - \frac{1}{N} \sum_{i=1}^{n_e} \log(\xi_{e,i} - z) \\ &+ \frac{1}{N} \log(\Lambda) + \frac{2N - n_o - n_e}{N} \phi - \eta. \end{aligned} \quad (17)$$

The expression for the eigenvalue  $\Lambda$  of the transfer matrix (12) becomes

$$2 \log(\Lambda) = \sum_{i=1}^{n_o} \log(\xi_{o,i}) + \sum_{i=1}^{n_e} \log(\xi_{e,i}). \quad (18)$$

The Ansatz (60) together with the BAE (13) correctly give the eigenvector with eigenvalue (18) of the transfer matrix for *almost* all densities. The description fails for the two states in which the lattice is filled completely with either s- or l-walls. In these cases it is possible to have 'virtual' l- or s-walls respectively, running around the cylinder.

## 5 Thermodynamic limit

It is clear that for the largest eigenvalue we must have  $n_o = n_e$ . In that case the solution for  $\xi_{o,i}$  and  $\xi_{e,i}$  must be the same. If not, the largest eigenvalue would be degenerate which cannot be the case by the Perron-Frobenius theorem. We therefore from now on omit the subscripts o and e and we set

$n_o = n_e = n_s$ , as well as  $\xi_{o,i} = \xi_{e,i} = \xi_i$ . The roots  $\xi_i$  and  $\psi_j$  approach two curves in the complex plane (see Fig. 3). We shall refer to these curves as  $\Xi$  and  $\Psi$  respectively.

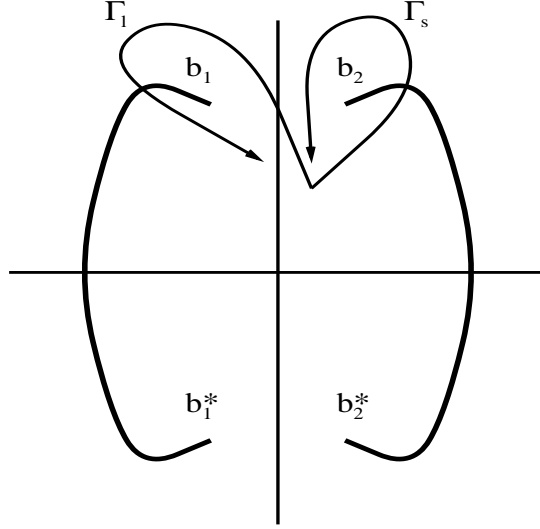


Figure 3: BAE curves.

From numerical calculations we note that there are no holes in the solution for the largest eigenvalue. Under the assumption that there are no holes in the thermodynamic limit of the solution we infer from the BAE (15) that for  $(N \rightarrow \infty)$

$$\frac{N + n_1}{2} f_s(\xi_k)(\xi_{k+1} - \xi_k) = 2\pi i, \quad (19)$$

$$N f_1(\psi_k)(\psi_{k+1} - \psi_k) = 2\pi i, \quad (20)$$

where  $f_s$  and  $f_1$  are the derivatives of the functions  $F_s$  and  $F_1$  respectively. These equations allow us to convert the sums in (16) and (17) into contour-integrals. By introducing the densities  $Q_1 = n_1/N$  and  $Q_s = n_s/N$  we obtain the following relations between  $f_s$  and  $f_1$  in the thermodynamic limit:

$$f_s(z) = \frac{1}{z} - \frac{2}{1 + Q_1} \frac{1}{2\pi i} \int_{b_1^*}^{b_1} \frac{f_1(\psi)}{z - \psi} d\psi, \quad (21)$$

$$f_1(z) = \frac{1}{z} + \frac{1+Q_1}{2\pi i} \int_{b_2^*}^{b_2} \frac{f_s(\xi)}{z-\xi} d\xi. \quad (22)$$

The points  $b_1, b_1^*, b_2$  and  $b_2^*$  are the thermodynamic limit points of  $\psi_1, \psi_{n_1}, \xi_{n_s}$  and  $\xi_1$ . From the form of equation (21) and (22) we see that  $f_s(z)$  is analytic along the contour  $\Gamma_s$ , though  $f_1(z)$  is not. The function  $f_1(z)$  differs on both sides of the curve  $\Xi$  by the amount

$$\frac{1+Q_1}{2\pi i} \oint_{|\xi-z_*|=\epsilon} \frac{f_s(\xi)d\xi}{z_*-\xi} = -(1+Q_1)f_s(z_*), \quad (23)$$

where  $z_*$  is the point where  $\Gamma_s$  crosses the curve  $\Xi$ . The analytic continuation of the function  $f_1(z)$  along  $\Gamma_s$  therefore equals the function  $f_1(z)+(1+Q_1)f_s(z)$ . A similar argument can be used for the analytic properties of the functions  $f_s$  and  $f_1$  along the contour  $\Gamma_1$ . The analytic properties of a linear combination  $G(z) = a_s f_s(z) + a_1 f_1(z)$  along the two contours are described by the so called monodromy operators  $\Gamma_s$  and  $\Gamma_1$ :

$$\Gamma_s : \begin{pmatrix} a_s \\ a_1 \end{pmatrix} \mapsto \begin{pmatrix} 1 & 1+Q_1 \\ 0 & 1 \end{pmatrix} \begin{pmatrix} a_s \\ a_1 \end{pmatrix}. \quad (24)$$

$$\Gamma_1 : \begin{pmatrix} a_s \\ a_1 \end{pmatrix} \mapsto \begin{pmatrix} 1 & 0 \\ -\frac{2}{1+Q_1} & 1 \end{pmatrix} \begin{pmatrix} a_s \\ a_1 \end{pmatrix}. \quad (25)$$

If the two curves close, i.e. they have the same limit point  $b_1 = b_2 = b$ , it is not possible to close the contours  $\Gamma_s$  and  $\Gamma_1$ . The only nontrivial closed curve is one that crosses both the curves  $\Xi$  and  $\Psi$ , so that we are left with only one monodromy operator:

$$\Gamma_1 \Gamma_s = \begin{pmatrix} 1 & 1+Q_1 \\ -\frac{2}{1+Q_1} & -1 \end{pmatrix}, \quad (26)$$

which has the property that  $(\Gamma_1 \Gamma_s)^4 = 1$ . This means that in this case the function  $G(z)$  is a single-valued function of the parameter

$$t(z) = \left( \frac{zb^{-1} - 1}{1 - b^{*-1}z} \right)^{\frac{1}{4}}, \quad z(t) = b \frac{1+t^4}{1+bb^{*-1}t^4}. \quad (27)$$

From now on we will write  $b = i|b|e^{i\gamma}$ . If we look at the orbit of  $f_1(z)$  under  $\Gamma_1 \Gamma_s$  we can see that  $f_1(z)$ ,  $(1+Q_1)f_s(z) - f_1(z)$ ,  $-f_1(z)$  and  $-(1+Q_1)f_s(z) +$

$f_1(z)$  belong to different sheets of the Riemann surface of the same function  $G$ , where  $G$  is given by (Appendix B):

$$G = \left( (e^{-i\pi/4}t + e^{i\pi/4}t^{-1}) - Q_l (e^{i\pi/4}t + e^{-i\pi/4}t^{-1}) \right) \frac{1}{2z(t)}. \quad (28)$$

## 6 Entropy

The knowledge of the function  $G$  allows us to calculate the eigenvalue from the BAE (15), see appendix C. Equations (1) and (4) show that the entropy per site for  $\Delta_{\text{ls}} = 0$  is given by:

$$\sigma_N = N^{-1} \log \Lambda - \frac{Q_s Q_l}{1 - Q_s} \eta. \quad (29)$$

This expression is precisely given by the solution (75) of the BAE.

At the QC-point,  $\gamma = 0, C = 0, \phi = 0$  (for the definition of  $C$ , see appendix B) and the domain wall densities given by (66) and (67) become

$$Q_l = \sqrt{2} - 1, \quad 2Q_s = 2 - \sqrt{2}. \quad (30)$$

This implies via (3) that the area per site  $A/N$  on the QC-point is given by

$$A/N = 12\sqrt{2} - 16, \quad Q_{\text{rect}} = 6 - 4\sqrt{2}, \quad Q_{\text{tri}} = 12\sqrt{2} - 16. \quad (31)$$

Therefore the entropy per area at the QC-point is given by

$$\begin{aligned} \sigma_{\text{a},0} = (A/N)^{-1} \sigma_N &= \frac{1 + \sqrt{2}}{2\sqrt{2}} \left( \log 4 - \sqrt{2} \log(1 + \sqrt{2}) \right) \\ &\approx 0.1193642186 \dots \end{aligned} \quad (32)$$

Away from the QC-point, there are two incommensurate phases. There is a two-fold degenerate four-fold symmetric phase in which one type of triangle (say the up and down pointing ones) dominates while the other type is suppressed. The triangles form rectangular and octagonal cells bounded by domain walls consisting of rectangles. Each orientation of the rectangles occurs equally often. A four-fold degenerate two-fold symmetric phase is present, if one type of rectangle dominates (say  $R_+$ , as in Fig. 1) forming

rectangular cells bounded by domain walls consisting of triangles. The 90 degrees rotated rectangle (here  $R_-$ ) is suppressed in this phase and the other two types of rectangle occur equally often, as well as both types of triangle.

Two independent parameters describe the deviations from the QC-point into these phases. The four-fold phase is described by the parameter  $\gamma$  which measures the difference in the densities of the two types of triangle. This phase also requires  $\Delta_{ls} = \partial \log \Lambda / \partial \phi = 0$ . The two-fold phase is described by  $\epsilon = \Delta_{\pm} / N = 1 - Q_1 - 2Q_s$ . This parameter measures the difference in densities of the  $\pm$  tilted rectangles, see equation (2). In this phase  $\phi = 0$  and  $\partial \log \Lambda / \partial \phi = 0$ .

## 6.1 Two-fold symmetric phase

In the two-fold phase  $\gamma = \Delta_{ls} = \phi = 0$  and the densities (66) and (67) become

$$\begin{aligned} Q_1 &= (\sqrt{2} - 1)(1 + 4\Re(C) + 4\Im(C)). \\ 2Q_s &= 2 - \sqrt{2} - 2\sqrt{2}\Re(C) + 2(2 - \sqrt{2})\Im(C). \end{aligned} \quad (33)$$

Using the fact that  $\delta_{ls}/N = Q_1\sqrt{2} - 2Q_s = 0$  in the two-fold phase,  $C$  can be expressed in  $\epsilon$ :

$$\Re(C) = \frac{\sqrt{2} - 1}{4\sqrt{2}}\epsilon, \quad \Im(C) = -\frac{2\sqrt{2} - 1}{4\sqrt{2}}\epsilon. \quad (34)$$

Since a nonzero value of  $\epsilon$  implies that  $C \neq 0$  it thus not only affects the value of the residues, or equivalently the densities, but also the topology of the Riemann surface of  $G$  (see appendix B). The formula (64) gives the lowest order corrections compatible with the modifications to the residues using the above value for  $C$ . It does not however take into account the changes in the topology. Those corrections become comparable with (64) when  $|b_1 - b_2|^{1/2} \sim \epsilon$  (see the end of appendix B). Since we want to know the corrections to the entropy density we need to know how small changes in the topology modify the integrals in appendix C. These corrections arise from the contributions of the poles at  $z = 0$  and  $z = \infty$  on other parts of the Riemann surface, which were previously disconnected. Since the net total residue on each part of the surface is zero, the lowest order correction to the integrals in appendix C will be of the order of  $|b_1 - b_2|^2 \sim \epsilon^4$ . The entropy

density is linear in the integrals of appendix C, the lowest order corrections to the entropy can therefore be calculated using the modifications to the residues only. The entropy per area up to second order in  $\epsilon$  then becomes:

$$\sigma_a = \sigma_{a,0} - \epsilon^2 \frac{1 + \sqrt{2}}{8} \left( \log 4 + \sqrt{2} \log(1 + \sqrt{2}) \right). \quad (35)$$

Comparing this expansion with the expression for  $\sigma_a$  in terms of the phason elasticity (8) one obtains for the elastic constants:

$$K_\mu \left( \sqrt{2} - 1 \right)^2 + K_\xi \sqrt{2} = \left( \sqrt{2} - 1 \right) \left( \log 4 + \sqrt{2} \log \left( 1 + \sqrt{2} \right) \right). \quad (36)$$

## 6.2 Four-fold symmetric phase

In the four-fold symmetric phase  $\epsilon = 0$ . In this case the entropy throughout the entire four-fold phase can be calculated exactly. First we note that  $\Delta_{\text{ls}} = \partial\Lambda/\partial\phi$ , which can be calculated analogously to the lowest order corrections in  $\epsilon$ . It is then found that

$$\frac{\partial\Lambda}{\partial\phi} \sim \frac{\partial\Lambda}{\partial C} \Big|_{C=0} = 0. \quad (37)$$

The densities in this case are

$$Q_1 = \left( 1 + \sqrt{2} \cos \frac{\gamma}{2} \right)^{-1} \left( 1 - \sqrt{2} \sin \frac{\gamma}{2} \right). \quad (38)$$

$$2Q_s = \left( 1 + \sqrt{2} \cos \frac{\gamma}{2} \right)^{-1} \left( \sqrt{2} \cos \frac{\gamma}{2} + \sqrt{2} \sin \frac{\gamma}{2} \right). \quad (39)$$

and the layer separation is

$$A/N = 1 - (\sqrt{2} - 1)^2 \frac{\sqrt{2} \cos \gamma/2 - 1}{\sqrt{2} \cos \gamma/2 + 1}. \quad (40)$$

The area fraction of triangles in terms of  $\gamma$  then can be written as

$$\alpha_t = \frac{Q_{\text{tri}}}{A/N} = (\sqrt{2} + 1) \frac{\sqrt{2} - \cos \gamma/2}{1 + \cos \gamma/2}, \quad (41)$$

so that the four-fold symmetric phase corresponds to  $1/2 \leq \alpha_t \leq 1$ . The entropy per area in this regime is found to have the following form

$$\begin{aligned} \sigma_a = & \frac{2 + \sqrt{2}}{4 \cos^2 \gamma/4} \left( \log \left( \frac{4}{\cos \gamma} \right) \right. \\ & + \cos \left( \frac{\pi}{4} + \frac{\gamma}{2} \right) \log \tan \left( \frac{\pi}{8} + \frac{\gamma}{4} \right) \\ & \left. + \cos \left( \frac{\pi}{4} - \frac{\gamma}{2} \right) \log \tan \left( \frac{\pi}{8} - \frac{\gamma}{4} \right) \right). \end{aligned} \quad (42)$$

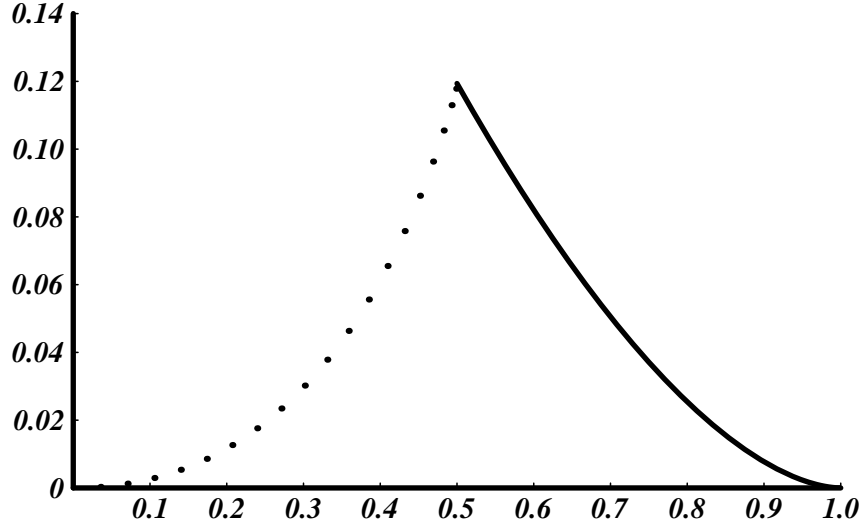


Figure 4: Entropy as a function of  $\alpha_t$ . Solid line corresponds to the exact solution. Dots are numerical results for  $N=198$ .

Expanding  $\sigma_a$  up to lowest order in  $\gamma$  yields

$$\sigma_a = \sigma_{a,0} - \gamma^2 \frac{1 + \sqrt{2}}{32\sqrt{2}} \left( 4 - \log 4 - \sqrt{2} \log \left( 1 + \sqrt{2} \right) \right). \quad (43)$$

To compare this with the phason strain description we note that in lowest order in  $\gamma$

$$\delta_{ls}/L = -\frac{\gamma(\sqrt{2} + 1)}{4}. \quad (44)$$

Using (10) and (8) we then find that

$$\begin{aligned} 4K_\mu - K_\xi &= \frac{\sqrt{2}-1}{\sqrt{2}} \left( 4 - \log 4 - \sqrt{2} \log(1 + \sqrt{2}) \right) \\ &\approx 0.4004597643\dots \end{aligned} \tag{45}$$

Combining (36) and (45) one obtains the phason elastic constants:

$$K_\mu = 4(\sqrt{2}-1)^3 \approx 0.2842712475\dots \tag{46}$$

$$\begin{aligned} K_\xi &= \frac{\sqrt{2}-1}{\sqrt{2}} \left( \log 4 + \sqrt{2} \log(1 + \sqrt{2}) - 4(\sqrt{2}-1)^4 \right) \\ &\approx 0.7366252255\dots \end{aligned} \tag{47}$$

Qualitatively, this octagonal tiling displays the same behavior as the square-triangle tiling.<sup>(8)</sup> At  $\alpha_t = \frac{1}{2}$  the model undergoes a so-called anomalous first order transition. This means that at fixed density the derivative of the entropy w.r.t. to the density, i.e. the pressure, has a jump, see Fig. 4. This then provides a mechanism for locking on the quasi-crystal phase over a range of pressures.

## 7 Conclusion

In this paper we successfully applied Bethe Ansatz to the square hexagon random tiling model. This model is a physical,<sup>(12)</sup> or atomistic, model of a quasi-crystal with eight-fold rotational symmetry. Amongst other things its solution answers the question posed in<sup>(7)</sup> if the random tiling hypothesis would hold for this model. It remains unclear however, what the precise conditions for solvability of these tiling models are. In this respect, the irrotationality constraint, which is satisfied by both the square-triangle and the square-hexagon tiling, might be an important guide. Such a constraint, not necessarily irrotationality, which reduces the degrees of freedom probably has some influence on the integrability. The tenfold tiling by rectangles and triangles<sup>(13)</sup> however does admit a Bethe Ansatz. We know not of any constraint for this tiling, nor have we solved the Bethe Ansatz equations. In the future we hope to present some numerical results for this tiling.



## Acknowledgment

This research was supported by FOM, which is part of the Dutch Foundation for Scientific Research NWO.

## A Bethe Ansatz

In this section we show how to set up an Ansatz for the eigenvectors of the transfer matrix  $\mathbf{T}$  to solve the eigenvalue problem. The conserved quantities make  $\mathbf{T}$  block-diagonal. We can make use of this fact by diagonalizing  $\mathbf{T}$  in each sector separately. It is helpful to start with the easiest sectors  $2n_s = 0, 1$ ,  $n_l = 0, 1$ . Later we generalize the method to arbitrary values of  $2n_s$ ,  $n_l$ .

### A.1 Domain walls of one kind only

The sectors where either  $n_l = 0$  or  $n_s = 0$  are very simple. E.g., in a sector with  $n_l = 0$ ,  $\mathbf{T}$  just shifts all s-walls one step to the right. If we assign a wave-vector  $p_i$  to every s-wall and denote the coordinate of the  $i$ th s-wall by  $x_i$ , the eigenvectors  $\psi(\{x_i\})$  of  $\mathbf{T}$  in these sectors can be written as a product of plane waves:

$$\psi(\{x_i\}) = \prod_{i=1}^{2n_s} e^{-ip_i x_i}. \quad (48)$$

The eigenvalue in terms of the wave-vectors is:

$$\Lambda = \prod_{i=1}^{2n_s} e^{ip_i}. \quad (49)$$

When using periodic boundary conditions the wave-vectors have to obey the following equation:

$$e^{iNp_i} = 1. \quad (50)$$

These equations are easily solved to give the spectrum of  $\mathbf{T}$  in these sectors. For later convenience we will fix some notation. The wave-vectors for the l-walls will be called  $q_j$  and in the following we will make frequently use of the exponentiated momenta  $u_i = \exp(ip_i)$  and  $w_j = \exp(iq_j)$ .

## A.2 The sector $n_l = 1, 2n_s = 1$ .

The simplest non-trivial sector is that with one s- and one l-wall, see Fig. 5. Let  $z$  be the coordinate of the l-wall, the eigenvalue equations then read:

$$\Lambda\psi(x; z) = \psi(x-1; z), \quad x > z+1. \quad (51)$$

$$\Lambda\psi(x; z) = \psi(x-1; z), \quad x < z. \quad (52)$$

$$\Lambda\psi(x+1; x) = e^{(\eta-\phi)/2}\psi(x; x) + e^\phi\psi(x-1; x). \quad (53)$$

$$\Lambda\psi(x; x) = e^{(\eta-\phi)/2}\psi(x; x+1). \quad (54)$$

We do not have to specify exactly the positions of the walls in the intermediate state  $\psi(x; x)$  when the walls cross via  $R_s$ . We only denote this state by  $\psi(x; x)$  which we can express in  $\psi(x; x+1)$  with equation (54).

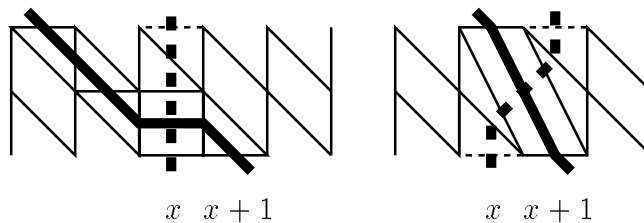


Figure 5: Crossings of two domain walls.

We can solve this eigenvalue problem by making the following plane wave Ansatz for the eigenfunction

$$\begin{aligned} \psi(x; z) &= A(\rho, \pi)u_\pi^{-x}w_\rho^{-z}, \quad x > z. \\ \psi(x; z) &= A(\pi, \rho)u_\pi^{-x}w_\rho^{-z}, \quad x < z. \end{aligned} \quad (55)$$

From this Ansatz, in which we have introduced the auxiliary labels  $\pi$  and  $\rho$  for later convenience, follow the eigenvalue and the relation between the two amplitudes before and after the collision

$$\begin{aligned} \Lambda &= u_\pi, \quad A(\rho, \pi) = S_{\text{ls}}(\rho, \pi)A(\pi, \rho). \\ S_{\text{ls}}(\rho, \pi) &= (e^\phi u_\pi + e^{\eta-\phi} u_\pi^{-1} w_\rho^{-1}). \end{aligned} \quad (56)$$

If we take periodic boundary conditions we get the following equations for the complex numbers  $u_\pi$  and  $w_\rho$ :

$$\begin{aligned} u_\pi^N &= \frac{A(\rho, \pi)}{A(\pi, \rho)} = S_{\text{ls}}(\rho, \pi). \\ (u_\pi w_\rho)^N &= 1. \end{aligned} \quad (57)$$

One can check that for arbitrary  $n_l$  and  $2n_s = 1$ , the eigenvector is given by

$$\psi(x; z_1, \dots, z_{n_l}) = \sum_{\rho} A(\Gamma) u_\pi^{-x} \prod_{k=1}^{n_l} w_{\rho_k}^{-z_k}, \quad \Lambda = u_\pi. \quad (58)$$

Here we have introduced a shorthand notation  $\Gamma$  for the dependency of the amplitude on the permutation  $\rho$  and the order of types of domain walls. This information is coded in the following way. Let  $\mathbf{r}$  be the vector of coordinates  $x, z_k$  of all domain walls, ordered so that  $r_m < r_{m+1}$ . The entries of the vector  $\Gamma$  are the elements of the permutation  $\rho$  together with the auxiliary label  $\pi$ . The order of succession in  $\Gamma$  of  $\pi$  and elements taken from  $\rho$  matches that of  $x$  and the  $z_k$ 's in  $\mathbf{r}$ , like in equation (55)

Amplitudes differing in an exchange of neighboring s- and l-walls or an exchange of two neighboring l-walls are related by the scattering matrix elements  $S_{\text{ls}}(\rho_k, \pi)$  (56) and  $S_{\text{ll}}(\rho_k, \rho_l)$  respectively, where  $S_{\text{ll}}(\rho_k, \rho_l) = -1$  for  $k \neq l$ . Imposing periodic boundary conditions gives us the BAE for these sectors:

$$\begin{aligned} u_\pi^N &= \frac{A(\rho_1, \dots, \rho_{n_l}, \pi)}{A(\pi, \rho_1, \dots, \rho_{n_l})} = \prod_{k=1}^{n_l} S_{\text{ls}}(k, \pi). \\ w_k^{-N} &= S_{\text{ls}}(k, \pi) \prod_{j \neq k=1}^{n_l} S_{\text{ll}}(k, j) = (-)^{n_l-1} S_{\text{ls}}(k, \pi). \end{aligned} \quad (59)$$

### A.3 Sectors with arbitrary values of $n_s$ and $n_l$

Let  $z$  be the coordinate of the l-wall and  $x_i$  the coordinates of the  $i$ th s-walls. By letting  $t$  be the vertical coordinate and  $c_i$  the number of l-walls to the left of the  $i$ th s-wall, we see that  $(x_i + t + c_i \bmod 2)$  is a conserved quantity for every s-wall. This means that the s-walls split up into two kinds: odd and even ones. We shall therefore change our notation a little bit:  $x_i$  and  $y_j$  will

denote the coordinate of the  $i$ th odd and the  $j$ th even s-wall respectively. Their total numbers will be denoted by  $n_o$  and  $n_e$  and  $2n_s = n_o + n_e$  and we shall use the shorthand  $S_{o,e}$  for  $S_{s_o,s_e}$ .

The Ansatz for the eigenvector in a general sector is given by:

$$\psi(x_1, \dots, x_{n_o}; y_1, \dots, y_{n_e}; z_1, \dots, z_{n_1}) = \sum_{\pi} \sum_{\mu} \sum_{\rho} A(\Gamma) \prod_{i=1}^{n_o} u_{\pi_i}^{-x_i} \prod_{j=1}^{n_e} v_{\mu_j}^{-y_j} \prod_{k=1}^{n_1} w_{\rho_k}^{-z_k}, \quad (60)$$

with eigenvalue

$$\Lambda = \prod_{i=1}^{n_o} u_i \prod_{j=1}^{n_e} v_j. \quad (61)$$

It turns out that in higher sectors all relations factorize into two-domain wall scattering relations, like (56). The BAE for  $u_i$ ,  $v_j$  and  $w_k$  using periodic boundary conditions then are

$$\begin{aligned} u_i^N &= \prod_{\substack{m=1 \\ m \neq i}}^{n_o} S_{o,o}(i, m) \prod_{j=1}^{n_e} S_{o,e}(i, j) \prod_{k=1}^{n_1} S_{1o}(k, i). \\ v_j^N &= \prod_{i=1}^{n_o} S_{o,e}(i, j) \prod_{\substack{m=1 \\ m \neq j}}^{n_e} S_{e,e}(j, m) \prod_{k=1}^{n_1} S_{1e}(k, j). \\ w_k^{-N} &= \prod_{i=1}^{n_o} S_{1o}(k, i) \prod_{j=1}^{n_e} S_{1e}(k, j) \prod_{\substack{m=1 \\ m \neq k}}^{n_1} S_{11}(k, m). \end{aligned} \quad (62)$$

Here,  $S_{1o}$  is given by (56) as well as  $S_{1e}$  with  $u$  replaced by  $v$ . Furthermore,

$$S_{11} = S_{o,o} = S_{e,e} = -1, \quad S_{o,e} = 1. \quad (63)$$

## B Calculation of the function $G$

In the following we will always assume that the two curves have the same limit point. In this case the Riemann surface of the function  $G$  becomes disconnected and consists of an infinite number of discrete parts comprising four sheets each. Each of these parts can be mapped onto the plane by (27). We fix a particular part and sheet of the Riemann surface by choosing  $G$

equal to  $f_1$  at  $z = 0$ , on the sheet with the point  $t = e^{i\pi/4}$ . The form of  $G$  on the other sheets of this part of the Riemann surface is then determined by the monodromy operators  $\Gamma_s$  and  $\Gamma_l$ . The finiteness of the densities  $Q_s$  and  $Q_l$  implies that the forms  $f_s(z)dz$  and  $f_l(z)dz$  are non-divergent at  $z = b$  and  $z = b^*$ . The only singularities therefore are the simple poles at  $z = 0$  and  $z = \infty$ . The residues of  $Gdz$  at these points can be easily calculated from  $f_1$  and its monodromy using equation (26). They are listed in Table 1. From this table we see that the functions  $f_1$ ,  $(1 + Q_l)f_s - f_1$ ,  $-f_1$  and  $-(1 + Q_l)f_s + f_1$  belong to the different sheets of the same part of the Riemann surface of the function  $G$ .

$z$	$t_n$	$G$	$r_n$
0	$e^{i\pi/4}$	$f_1$	1
$\infty$	$ie^{-i\gamma/2}$	$(1 + Q_l)f_s + f_1$	$Q_l + 2Q_s - 2$
0	$-e^{-i\pi/4}$	$(1 + Q_l)f_s - f_1$	$Q_l$
$\infty$	$-e^{-i\gamma/2}$	$-f_1$	$1 - 2Q_s$
0	$-e^{i\pi/4}$	$-f_1$	-1
$\infty$	$-ie^{-i\gamma/2}$	$-(1 + Q_l)f_s - f_1$	$2 - Q_l - 2Q_s$
0	$e^{-i\pi/4}$	$-(1 + Q_l)f_s + f_1$	$-Q_l$
$\infty$	$e^{-i\gamma/2}$	$f_1$	$2Q_s - 1$

Table 1: Poles and residues of  $Gdz$

The form  $Gdz$  is defined unambiguously by its residues and equals

$$\begin{aligned}
Gdz &= \sum_{n=1}^8 \frac{r_n}{t - t_n} dt \\
&= \left( \frac{1}{2} (e^{-i\pi/4}t + e^{i\pi/4}t^{-1}) - \frac{Q_l}{2} (e^{i\pi/4}t + e^{-i\pi/4}t^{-1}) + \right. \\
&\quad \left. + C(t + t^{-3}) + C^*(t^{-1} + t^3) \right) \frac{1}{z(t)} \frac{dz(t)}{dt} dt. \tag{64}
\end{aligned}$$

where  $C$  given by

$$C = \frac{1}{2(1 + e^{2i\gamma})} \left( -(1 - Q_l) (ie^{i\gamma/2} + e^{i\pi/4}) \right)$$

$$+ (1 - 2Q_s)(1 - i)e^{i\gamma/2} + 2i \sin \frac{\pi}{4}. \quad (65)$$

Or equivalently, one can write the domain wall densities as functions of  $\gamma$  and  $C$ :

$$2Q_s = 1 - \cos\left(\frac{\pi}{4} + \frac{\gamma}{2}\right) + Q_1 \cos\left(\frac{\pi}{4} - \frac{\gamma}{2}\right) - 2\Re(C) \left(\cos \frac{\gamma}{2} + \cos \frac{3\gamma}{2}\right) + 2\Im(C) \left(\sin \frac{3\gamma}{2} - \sin \frac{\gamma}{2}\right). \quad (66)$$

$$Q_1 = \left(1 + \sqrt{2} \cos \frac{\gamma}{2}\right)^{-1} \left(1 - \sqrt{2} \sin \frac{\gamma}{2} + 2\Re(C) \left(\cos \frac{3\gamma}{2} + \cos \frac{\gamma}{2} + \sin \frac{3\gamma}{2} - \sin \frac{\gamma}{2}\right) + 2\Im(C) \left(\cos \frac{3\gamma}{2} + \cos \frac{\gamma}{2} - \sin \frac{3\gamma}{2} + \sin \frac{\gamma}{2}\right)\right). \quad (67)$$

The monodromy properties of the curves  $\Xi$  and  $\Psi$  only hold when  $b_1 = b_2$ . These curves are defined by the form  $Gdz$  taking only purely imaginary values on the tangential vectors of  $\Xi$  and  $\Psi$ , see equations (19) and (20). Given the initial conditions these solutions must be unique except precisely at the points  $t = 0$  and  $t = \infty$ . At these points the different solutions should meet. If this were not the case the curves would intersect or would not close, destroying the assumed monodromy assumption. The condition  $\Re(Gdz) = 0$  must therefore be satisfied identically at the points  $t = 0$  and  $t = \infty$ . From (64) and (27) it follows that

$$\begin{aligned} G \frac{dz}{dt} \Big|_{t=0} &= 4C(1 + e^{2i\gamma})dt \Big|_{t=0} \\ G \frac{dz}{dt} \Big|_{t=\infty} &= -4C^*(1 + e^{-2i\gamma}) \frac{dt}{t^2} \Big|_{t=\infty} \end{aligned} \quad (68)$$

The monodromy assumption translates itself therefore in the condition  $C = 0$ . The Riemann surface of  $G$  then has infinitely many disconnected parts with four sheets each. If  $b_1 \neq b_2$  these parts become joined by regions of size  $|b_1 - b_2|$ . One can still use the variable  $t$  with  $b = (b_1 + b_2)/2$ . The function  $G$  then is single-valued except for the regions around  $t = 0$  and  $t = \infty$  where  $|t| \sim |b_1 - b_2|^{1/4}$  or  $|t|^{-1} \sim |b_1 - b_2|^{1/4}$  respectively. Equation (64) gives the corrections to the changes in the values of the residues if  $C \neq 0$ . It does

not however take into account contributions arising from the changes in the topology of the Riemann surface. For small  $t$  the form  $Gdz$  is approximated by terms of the order of  $t^2dt$  and  $Cdt$ . As a lowest order approximation (64) thus is valid if  $|t|^2 \sim |b_1 - b_2|^{1/2} < C$ .

## C Calculation of $\Lambda$

In order to remove singularities at  $z = 0$  and  $z = \infty$  occurring in some of the expressions in this appendix, we introduce the following forms:

$$\begin{aligned}
g_1 dz &= \left( \frac{r_4}{t - t_4} + \frac{r_8}{t - t_8} \right) dt \\
g_s dz &= \left( \frac{r_2}{t - t_2} + \frac{r_6}{t - t_6} \right) dt \\
h_1 dz &= \left( \frac{r_1}{t - t_1} + \frac{r_5}{t - t_5} \right) dt \\
h_s dz &= \left( \frac{r_3}{t - t_3} + \frac{r_7}{t - t_7} \right) dt
\end{aligned} \tag{69}$$

The BAE (15) allow us to evaluate the following expression using the definition  $F_1$  as given by equation (17).

$$\begin{aligned}
J_{1,\infty} &= \Re \int_b^\infty (f_1 - g_1) dz \\
&= \Re \lim_{t \rightarrow t_8} (F_1(z(t)) - r_4 \log(t - t_4) - r_8 \log(t - t_8)) \\
&= (1 - 2Q_s) \log \frac{|b| |\cos \gamma|}{4} + N^{-1} \log \Lambda + 2(1 - Q_s)\phi - \eta. \tag{70}
\end{aligned}$$

The equality sign on the second line follows from the fact that  $F_1(z)$  is a primitive function of  $f_1(z)$  and that  $b$  is a solution of the BAE (15). The expression on the third line follows from the definition of  $F_1(z)$  as given by equation (17). Similarly we find using also the definition for  $F_s(z)$ , equation (16),

$$J_{s,\infty} = \Re \int_b^\infty ((1 + Q_1)f_s + f_1 - g_s) dz$$

$$= (2 - Q_1 - 2Q_s) \log \frac{|b| |\cos \gamma|}{4} + N^{-1} \log \Lambda + 2(1 - Q_1 - Q_s)\phi - \eta. \quad (71)$$

$$\begin{aligned} J_{1,0} &= \Re \int_b^0 (f_1 - h_1) dz \\ &= \log \frac{4|b|}{|\cos \gamma|} - N^{-1} \log \Lambda + 2(1 - Q_s)\phi - \eta. \end{aligned} \quad (72)$$

$$\begin{aligned} J_{s,0} &= \Re \int_b^0 ((1 + Q_1)f_s - f_1 - h_s) dz \\ &= Q_1 \log \frac{4|b|}{|\cos \gamma|} + N^{-1} \log \Lambda - 2s_1 - 2(1 + Q_1 - Q_s)\phi + \eta. \end{aligned} \quad (73)$$

with

$$s_1 = N^{-1} \sum_{j=1}^{n_1} \log \psi_j. \quad (74)$$

Eliminating  $|b|$ ,  $\phi$  and  $s_1$  from the equations (70)–(73) we find for the eigenvalue  $\Lambda$  and the chemical potential  $\eta$

$$\begin{aligned} N^{-1} \log \Lambda - \eta \frac{Q_s Q_1}{1 - Q_s} &= Q_s J_{s,\infty} + \frac{1}{2} \left( 1 - 2Q_s + \frac{Q_s Q_1}{1 - Q_s} \right) J_{1,\infty} \\ &\quad - \frac{1}{2} \left( 1 - \frac{Q_s Q_1}{1 - Q_s} \right) J_{1,0} - \left( 1 - \frac{Q_s Q_1}{1 - Q_s} \right) \log \frac{\cos \gamma}{4}. \end{aligned} \quad (75)$$

On the other hand, the integrals  $J_{1,\infty}$  and  $J_{s,\infty}$  can easily be integrated in the  $t$ -plane using the results of appendix B.

$$J_{1,\infty} = \sum_{n \neq 4,8}^8 r_n \log |t_n - t_8|. \quad (76)$$

$$J_{s,\infty} = \sum_{n \neq 2,6}^8 r_n \log |t_n - t_2|. \quad (77)$$

With the help of Table 1 of appendix B these expressions are given explicitly by

$$J_{1,\infty} = \frac{1}{2} \log \left| \frac{1 - \cos(\pi/4 + \gamma/2)}{1 + \cos(\pi/4 + \gamma/2)} \right| + \frac{Q_1}{2} \log \left| \frac{1 + \cos(\pi/4 - \gamma/2)}{1 - \cos(\pi/4 - \gamma/2)} \right|. \quad (78)$$



$$J_{s,\infty} = \frac{1}{2} \log \left| \frac{1 - \cos(\pi/4 - \gamma/2)}{1 + \cos(\pi/4 - \gamma/2)} \right| + \frac{Q_1}{2} \log \left| \frac{1 - \cos(\pi/4 + \gamma/2)}{1 + \cos(\pi/4 + \gamma/2)} \right|. \quad (79)$$

And similarly  $J_{1,0}$  and  $J_{s,0}$  give:

$$J_{1,0} = \frac{1}{2}(2 - Q_1 - 2Q_s) \log \left| \frac{1 + \cos(\pi/4 - \gamma/2)}{1 - \cos(\pi/4 - \gamma/2)} \right| + \frac{1}{2}(1 - 2Q_s) \log \left| \frac{1 + \cos(\pi/4 + \gamma/2)}{1 - \cos(\pi/4 + \gamma/2)} \right|. \quad (80)$$

$$J_{s,0} = \frac{1}{2}(2 - Q_1 - 2Q_s) \log \left| \frac{1 + \cos(\pi/4 + \gamma/2)}{1 - \cos(\pi/4 + \gamma/2)} \right| \quad (81)$$

$$+ \frac{1}{2}(1 - 2Q_s) \log \left| \frac{1 - \cos(\pi/4 - \gamma/2)}{1 + \cos(\pi/4 - \gamma/2)} \right|. \quad (82)$$

Combining (78)–(82) and (75) then gives the eigenvalue expressed in the densities (given by (66) and (67)), the chemical potential  $\eta$  and the parameter  $\gamma$ .

## References

1. H.W.J. Blöte and H.J. Hilhorst, *J. Phys. A: Math. Gen.* **15**, L631 (1982).
2. D. Shechtman et al., *Phys. Rev. Lett.* **53**, 1951 (1984).
3. D. Levine and P.J. Steinhardt, *Phys. Rev. Lett.* **53**, 2477 (1984).
4. M. Widom et al., *Phys. Rev. Lett.* **63**, 310 (1989).
5. R. Collins, *Proc. Phys. Soc.* **83**, 553 (1964).
6. H. Kawamura, *Prog. Theor. Phys.* **70**, 352 (1983).
7. E. Cockayne, *J. Phys. A: Math. Gen.* **27**, 6107 (1994).
8. M. Widom, *Phys. Rev. Lett.* **70**, 2094 (1993).
9. P.A. Kalugin, *J. Phys. A: Math. Gen.* **27**, 3599 (1994).

10. C.L. Henley, In *Quasicrystals: The State of the Art*, P.J. Steinhardt and D.P. DiVincenzo eds., World Scientific, Singapore, 429 (1991).
11. J. de Gier and B. Nienhuis, *Phys. Rev. Lett.* **76**, 2918 (1996).
12. M. Oxborrow and C.L. Henley, *Phys. Rev.* **48B**, 6966 (1993).
13. M. Oxborrow and M. Mihalkovič, In *Proceedings of the International Conference on Aperiodic Crystals*, G. Chapuis and W. Paciorek eds., 178, Les Diablerets Switzerland, (1994).